©Freund Publishing House Ltd. International Journal of Nonlinear Sciences & Numerical Simulation, 10(11): 1655-1661, 2009

A hybrid approach to quantify lamination of the cerebral cortex

Oliver Schmitt[1], Harald Birkholz[2]

[1] *Department of Anatomy, University of Rostock, 18055, Rostock, Germany*
Email: schmitt@med.uni-rostock.de
[2] *Department of Mathematics, University of Rostock, 18057, Rostock, Germany*

Abstract

Alterations of cytoarchitectonic (CA) patterns in digital images of histological sections of the human cerebral cortex (CX) might indicate changes of brain functions. These lamination patterns can be extracted by calculating orthogonal testlines through CX by a stepwise scanning. 3D CA data of whole human brains at a histological resolution are not available and 2D sections deliver partial information only. The problem is to find an optimal method of scanning producing a minimum of distortions and noise by the transformation of the curvilinear CX to a rectangular presentation of CA layering. So far, the cortical surfaces are modeled as electrically charged regions to use the resulting field lines as testlines. However, local information of cell distributions was not considered. A hybrid approach constructs significantly better testlines in CX images with mixtures of columnar rich (local orientation rich) and orientation poor parts of strongly curved regions. The new hybrid approach is based on combining streamlines of the electric field with the structure tensor and constrained anisotropic diffusion. In addition, the introducing of projective transformations yields a significant improvement of cortical fingerprints. The statistical evaluation of the new method turns out to be robust with respect to artifacts and low local orientation information. The new technique can be generalized and applied to many different types of CX with local orientation information.

Keywords: cerebral cortex, brainmapping, traverses, transcortical scanning, local orientation, coherency, anisotropic diffusion, electric field.

1. Introduction

The human cerebral cortex (CX) is comparable with a topological envelope of gray matter covering a core of white matter. This gray matter of the cortical mantle is striped by a distinct internal lamination determined genetically [1] that can be subdivided by different parcellation schemes based on visualizations like CA in dgitial images [2]. The layered tissue is composed of different types of cells distributed inhomogeneously. Changes of this lamination pattern strongly suggest differences in brain subfunctions [3]. To detect regional alterations of the lamination the CX can be sampled by orthogonal testlines (traverses) of succeeding points on the cortical surface providing distributions of pixel intensities (profiles) [4, 5]. Each profile is registered in a profile array for statistical evaluation. The paths of these traverses is critical with regard to distortion of resulting profiles and there statistical evaluation [6]. Traverses are calculated by electrodynamic (ED) simulation between the upper and lower cortical surface. So far, cell columns running relatively perpendicular to the lamination have not been considered to support the calculation of traverses. The integration of local orientation in the calculation of testlines may have the advantage of reducing distortion of profiles. In this contribution we addressed the problem of combining the ED approach and a local orientation evaluation of cell distribution in a hybrid method. Advantages of this new technique have been evaluated statistically.

2 Material

For testing and comparing the new approach 20 μm thick human brain sections stained with a silver staining are used. Sections are digitized using a transparent flatbed scanner Nexscan F4100 (Heidelberger) providing a resolution of 5.04 μm per pixel with an 8 Bit dynamic.

3 Motivation and Notation

These 2D (scalar-valued) images are modeled by the continuous function $f : \mathbb{R}^2 \to \mathbb{R}$ with compact support. An image is supplemented with a manually defined region of interest $\Omega \subset \mathbb{R}^2$ with topological gender 0 or 1. For the ease of notation we restrict to the first case. The ROI is the area between two contours $H,L \subset \partial\Omega$, which represent the boundary of the gray matter. To cope with the geometry of Ω, traverses are computed. They define a transformation of $f|_\Omega$ into a cortical fingerprint. Traverses should exhibit the following properties: (1) A traverse is a curve from H to L. (2) Different traverses do not intersect. (3) Traverses cross the layers of the gray matter locally orthogonal. The properties (1) and (2) are achieved with the ED model [4]. It entirely relies on the manually defined contours, which are modeled as electrically charged, inducing a force field that drives mobile charges across the ROI. The trace of a charge that starts near a contour is used as a traverse. This is computationally efficient and reliable. The catch is that the property (3) is only achieved for the outermost layers. For a given f image it is possible to stabilize the ED model against bias of manual input by including the image into the input by including the image into the traverse generation algorithm to fulfill the property (3). For an estimation of the orientation locally orthogonal to gray-matter layers, neural columns are estimated. Along these line-like structures f is assumed to be smoother in comparison to the otherwise relatively random distribution and layered neurons. Column-like anisotropic structures are superposed by isotropic ones and laminations. The structure-tensor (a gradient-based low-level feature) can estimate the anisotropy. The estimation must be enhanced by thresholding excluding random anisotropy that does not originate from neural columns. We write for any $M,N \in \mathbb{N}$ and any feature $h \in L^1(\mathbb{R}^2, \mathbb{R}^{M\times N})$:

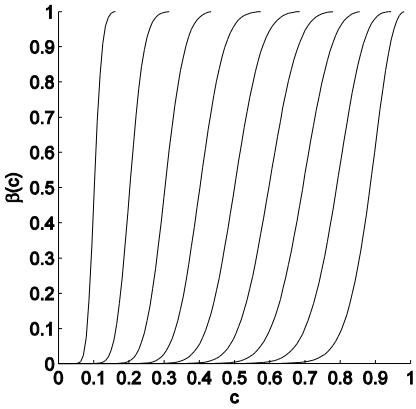

Fig.1: β as a sigmoid function of $c \in [0,1]$ for $\vartheta \in \{0.1, 0.2,\ldots, 0.9\}$ and constant s = 16.

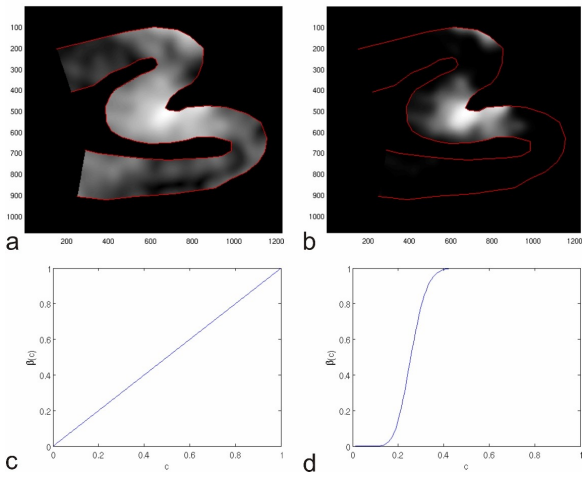

Fig. 2: .a) The normal coherency c as a special case of β with $\vartheta \in (0,1)$ and $s = 1$. b) β of the image function with $\vartheta = 0.2$, $s = 16$. In c) (for β with $\vartheta \in (0,1)$) and d) (for $\vartheta = 0.2$, $s = 16$) the increasing Beta-function for pointwise coherency enhancement is shown.

$$h_\sigma := \begin{pmatrix} h_{11} * G_\sigma & \cdots & h_{1N} * G_\sigma \\ \vdots & & \vdots \\ h_{M1} * G_\sigma & \cdots & h_{MN} * G_\sigma \end{pmatrix}$$

with $\sigma > 0$ and $h_0 := h$, where $G_\sigma(x) = \frac{1}{2\pi\sigma^2} exp\left(-\frac{\|x\|^2}{2\pi\sigma^2}\right)$ is a Gaussian kernel and $*$: $L^1(\mathbb{R}^2) \times L^1(\mathbb{R}^2) \to L^1(\mathbb{R}^2)$ is the convolution. The feature h is smoothed to an extent σ. The spacial argument is omitted in the following formulas. All features are meant pointwise evaluated. We write the structure tensor J of an absolute integrable function u: $\mathbb{R}^2 \to \mathbb{R}$

$$J := (\nabla u_\varepsilon (\nabla u_\varepsilon)^T)_\rho \qquad \varepsilon, \rho \geq 0.$$

This is the outer product of a smoothed gradient ∇u_s, itself smoothed component-by-component. J is symmetric and positive semidefinite. The eigenvalues of J are nonnegative, because they are before componentwise smoothing, and the subsequent averaging preserves this property. Let $\lambda_1 \geq \lambda_2 \geq 0$ be the eigenvalues of J with eigenvectors $\nu_1, \nu_2 \in \mathbb{R}^2$. In case $\lambda_1 > \lambda_2$ the eigenvector ν_1 exposes the orientation of the greatest local gray value variation. The vector ν_2 is orthogonal to ν_1 and thus indicates an orientation of greatest local smoothness of u. If $\lambda_1 = \lambda_2$ the eigenvectors of J are arbitrary. Thus the difference $\lambda_1 - \lambda_2$ is a measure for the accuracy of the orientation estimation encoded in ν_1 and ν_2. It is used smoothly normalized and called *coherence* c [8]:

$$c := \frac{\lambda_1 - \lambda_2}{\lambda_1 + \lambda_2 + \varepsilon}, \qquad 0 < \varepsilon \ll 1.$$

The coherence can be regarded as a probability for the assumption that the underlying image u shows column-like structures in a ρ-neighborhood. To make sure these column-like structures are pillars, c is smoothly thresholded with the increasing Beta-function. Its parameters shape it sigmoid, with an inflection point at $\vartheta \in [0, 1]$ and a slope $s > 1$ at ϑ (Fig. 2). The result refers to a local probability β for the presence of neural columns of width σ with coherence greater than ϑ to a ρ-neighborhood:

$$\beta := \frac{1}{B(\mu, \nu)} \int_0^c \xi^{\mu-1}(1-\xi)^{\nu-1}\, d\xi,$$

with $\mu := s$ and $\nu := \frac{(1-\vartheta)(s-1)}{\vartheta} + 1$ and B the Beta-function. Obviously $\beta \equiv 0$ as ϑ approaches 1 provided $s > 1$. This will be important for the model because it is a generalization of the ED model [4]. It must be emphasized that not in each region of the CX proper cell orientations occur. If the orientation is large enough it will be strongly weighted and vice versa.

3.1 Coherence enhancing diffusion

Anisotropic diffusion (DF) is a nonlinear filter based on the numerical solution to the partial differential equation describing the process of DF [9, 10]. The coherence of an image is used for local orientation estimation. The idea is to smooth an image first into the direction it already is smoothest. Although this converges to a steady-state image, in between, there is an improvement of coherence. The visual impression of the intermediate results is flow-like and its value is twofold. Firstly, any line-like structures are enhanced, so the existence is no longer in question. Secondly, the greater coherence might help to get a better estimation of the anisotropy in the ROI. We solve a slightly modified coherence-enhancing DF scheme, to be found in [15]:

$$u_t = \nabla \cdot (D\nabla u) \quad \text{for } (t,x) \in (0, T_1) \times \Omega, u(0,x) = f(x) \quad \text{for } x \in \Omega,$$

with the given image $f(x)$ as initial condition and no flux across the boundary. The diffusivity $D : \mathbb{R}^2 \to \mathbb{R}^{2\times 2}$ is faithful to the common scheme with the slight modification that the flux is thresholded in order to enhance exclusively neural columns and leave other superposed structures untouched. Let

$$J = Q \begin{pmatrix} \lambda_1 & \\ & \lambda_2 \end{pmatrix} Q^T, \qquad Q \text{ orthogonal}$$

be the diagonalized structure tensor with $\lambda_1 \geq \lambda_2 \geq 0$. Then we set

$$D = Q \begin{pmatrix} \mu_1 & \\ & \mu_2 \end{pmatrix} Q^T$$

With $\mu_1 := \varepsilon$,

$$\mu_2 := \begin{cases} \varepsilon, & \lambda_1 = \lambda_2 \\ \varepsilon + (1-\varepsilon)\beta \exp\left(-\frac{1}{(\lambda_1 - \lambda_2)^2}\right), & \lambda_1 \neq \lambda_2 \end{cases}$$

where $0 < \varepsilon \ll 1$. With this construction of D, the initial value problem is well-posed and delivers a unique solution for all stopping times T_l. The most questionable part of the proof is the smoothness of D in J. This is granted by the smoothness of β in J.

3.2 Hybrid ED traverse generation

The curvilinear paths of traverses computed by the ED [4] or alternative approaches [11] do not necessarily achieve the condition (3) (see above). Since inner and outer contours contribute only partial data for determining local respectively layer-specific orientation, we can use the concept of local orientation [2, 12, 13]. CA cell columns [14] facilitate the determination of locally perpendicular traverses, however, they are not always visible due to tangential sectioning. In the case of low local coherency of orientation, the weight of the ED approach should increase and vice versa. Hence, the ED technique and the local orientation are weighted to a hybrid ED orientation approach (HY). An electric field $F : \mathbb{R}^2 \rightarrow \mathbb{R}^2$ drives charges one by one from the push contour H to the pull contour L, across Ω

$$F(x) := \int_H \frac{x-\xi}{\|x-\xi\|^3}\,d\xi + \int_L \frac{\xi-x}{\|\xi-x\|^3}\,d\xi$$

For the ED model the ODE:

$$\dot{y} = \frac{F(y)}{\|F(y)\|}, y(0) = y_0^k, y(t) \in \Omega$$

is solved for different y_0^k that are placed near the push-contour H resulting in curves similar to electrical field lines. Because the traverses exhibit an unsatisfying behavior in between the driving force of the charge is modified, so it moves preferably with the local orientation of neural pillars, which we assume to exhibit certain coherence. For this the structure tensor of the DF-enhanced image J with eigenvalues $\lambda_1 \geq \lambda_2 \geq 0$ is applied. The amplified coherence is given by β see above. The crucial directional information in $x \in \mathbb{R}^2$ is given by an eigenvector $P(x)$ of $J(x)$ to $\lambda_2(x)$, which encloses an acute angle with $F(x)$.

Then the traverse is created with a time integration of another ODE. We solve:

$$\dot{y} = \beta\frac{F(y)}{\|F(y)\|} + (1-\beta)\frac{P(y)}{\|P(y)\|}, y(0) = y_0^k, y(t) \in \Omega$$

Let T_2 be the time, when y reaches L, so that we can inductively define a family of traverses with length 1 by: $Y_k(t) := y(tT_2)$. The traverses are decomposed by $0 = t_0 < t_1 < \ldots < t_n = 1$ into a grid of quadrilaterals: $Y^{k,l} := Y_k(t_l)$, if the traverses are computed with an appropriate accuracy or density and n is great enough. The computation starts with the first and the last path followed by densifying the paths recursively.

3.3 Piecewice Projective Transformation

The derivation of the cortical fingerprint is the final purpose of the traverse computation. The pixels under each traverse can be transfered as a column into the fingerprint. However a piecewise planar projective transformation from the traverse into a template grid has advantages. Let $Q_{k,l} \subset \mathbb{R}^2,\ k = 0,\ldots,m-1, l = 0,\ldots,n-1$ be the quadrilateral with the corners $\{Y^{k,l}, Y^{k+1,l}, Y^{k,l+1}, Y^{k+1,l+1}\}$. We assume that it is convex. Values of the image at $Q_{k,l}$ are mapped to a template quadrilateral $R_{k,l}$, where $R_{k,l}$ is part of a matrix of quadrilaterals of the fingerprint. The mapping which we use for pairs of original and template quadrilaterals $Q, R,$ is the unique planar projective transformation

$$\Pi: Q \rightarrow R: \Pi(x_1, x_2) = \left(\frac{p_1x_1 + p_2x_2 + p_3}{p_7x_1 + p_8x_2 + 1}, \frac{p_4x_1 + p_5x_2 + p_6}{p_1x_7 + p_8x_2 + 1}\right)^{\mathrm{T}}$$

with eight degrees of freedom. The fingerprint is the composition of all image information under the transformation of respective pairs of quadrilaterals from the traverse and the template grid. This defines a continuous piecewise projective transformation implying three appealing advantages. We are free to choose the sampling rate by proper choice of the template grid. We obtain a measurement for the blurring or distortion (Fig. 3i and j) with the absolute determinant of the Jacobian matrix of Π, which is defined in both the fingerprint domain and in the image domain. Furthermore, the mapping is invertible to map any features

derived from the fingerprint back into the image geometry.

3.4 Quality and Parameters

The most important feature for the ED-, HY- and HD-traverses is a perpendicular crossing of lamination. As the layers cannot be extracted directly with any current computational method, we need to rely on manual input of ideal traverses. For simplicity we define only straight line traverses of visually average ideal orientation. In this way the visual improvement of the novel approach can be put into a figure, a kind of an average angular error α. Let

$$Z^j = \left(Z^{j,l}\right)_{l=0,1} \in H \times L,\ j = 0, \dots, m'$$

be the ideal traverse grid, and $(Y^{k,l})_{l=0,\dots,n} \in \Omega^n,\ k = 0, \dots, m$ the computed traverse grid. An interpolation of the ideal traverse grid is

$$Z^\kappa = \left(Z^{\kappa,l}\right)_{l=0,1} \qquad \kappa \in [0, m] \text{ with}$$

$$Z^{\kappa,l} = (\kappa - [\kappa])Z^{[\kappa],l} + (1 - (\kappa - [\kappa]))Z^{[\kappa]+1,l}$$

where $[\cdot]$ denotes the greatest integer smaller than the number. The traverse-segment between the nodes $Y^{k,l}$ and $Y^{k+1,l}$ is judged by the angle $\varphi_{k,l}$ that it encloses with Z^κ, where κ is chosen such that the lines cross in $\frac{Y^{k,l}+Y^{k,l+1}}{2}$.

Let E be the set of and $\#E$ the number of traverse-segments that can be judged this way. Angles $\varphi_{k,l}$ between the ideal and the computed traverse-segments are averaged (mean error α):

$$\alpha := \frac{1}{\#E} \sum_{(k,l)\in E} \varphi_{k,l}.$$

4 Optimal Parameters and Statistics

Based on the statistical comparisons, the HD approach shows the smallest α. By investigating the parameterse for controlling the coherency and the DF we found that parameters converge to similar values for the 4 basic CX curvatures. An optimal DF ϑ is 0.7 and the optimal DF s is 5.8. For the hybrid part (HY) an optimal hybrid ϑ of 0.41 and a hybrid s of 7.5 is determined. Statistical comparison of the α's of HD, ED and HY shows a significant difference (Fig. 4).

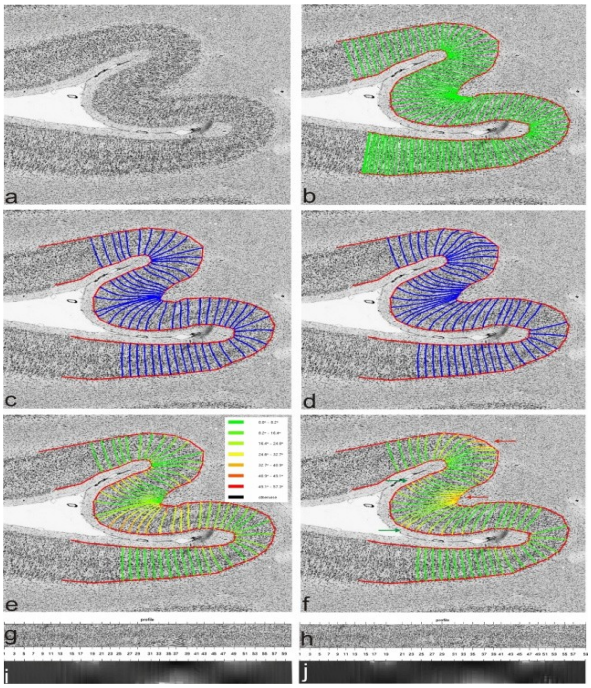

Fig. 3: a) Original image with a curved part of the CX. b) the ideal traverses (IT) in green. c) the EDT (blue). d) the HT (red). e) Comparison of EDT and IT. Green encodes small, red large angular errors. Mean angular error: 7.8°. f) Comparison of IT and HY (9.1°). Green arrows: stronger deviations from expected traverses, red arrows: regions with deviations not found in the EDT. g) EDT-fingerprint. h) HY-Fingerprint with distortions (arrow). i), j) that correspond to g), h) show the blurring derived from the determinant of the Jacobian of Π for all quadrilaterals.

5 Discussion

Orthogonal scanning is the first step of sampling the CX for statistical analysis [3, 5, 6] and the development of brain atlases. It is mandatory to optimize the scanning of CA to analyze a data structure containing minimal distortions. To obtain a profile reflecting an

almost unblurred progression of the CA, the sampling should be locally orthogonal to the cortical lamination. This is partially fulfilled by using coordinates of the cortical surfaces. However, most information is contained in the local distribution of cells. The ED model and local orientation of cells [17] were combined to calculate traverses. This approach guarantees reliable generation of traverses in those regions containing insufficient local orientation. Hence, the hybrid approach can be used in CX regions where strong cell columns occur as well as where those are absent. The local orientation can be enhanced by anisotropic DF filtering [9, 10, 15, 16] on CAs. Projective transformations reduce the sampling time and the blurring effect is diminished. In the past sampling was achieved by calculating neighboring testlines only [5], here a recursive subdivision of the ROI is realized. Finally, significantly lower deviations of the hybrid DF method with regard to ED were found.

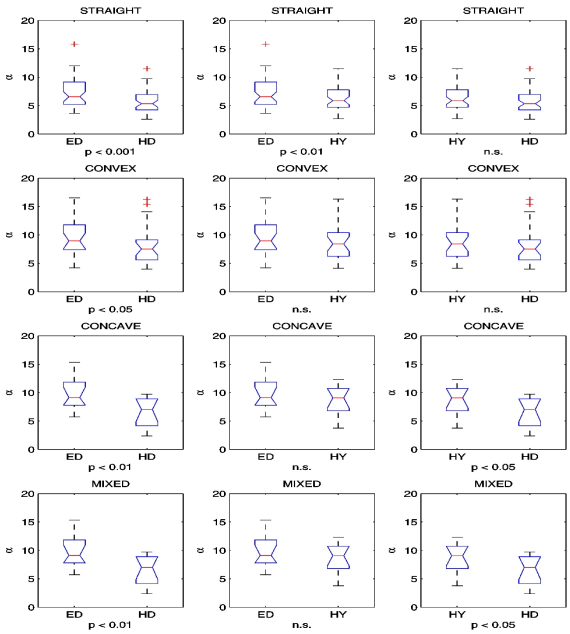

Fig. 4: Null hypotheses are tested of ED, HY and HD. A significant ($p \leq 0.05$) smaller α is found by HD with regard to HY and ED of straight, concave and mixed subregions. HY generates smaller values of α with respect to ED of straight and mixed subregions.

6 Conclusions

A new hybrid method following the intuitive visually recognizable CX borders combined with local cell distributions by methods of computer vision (anisotropic DF, local orientation), physical modeling (ED) and mapping (projective transformation) techniques was developed. The new anisotropic DF enhanced hybrid approach has a statistically significant smaller deviation to expert-defined ideal traverses of different curvatures in comparison to the ED or hybrid method without DF enhancement.

Acknowledgements

We thank Manfred Tasche (University of Rostock) for sharing his expertise and Martin Böhme (University of Lübeck) for his contributions. Especially, we thank Karl Zilles and Katrin Amunts (Jülich Research Center) for providing the brain sections.

References

[1] A Mallamaci, A Stoykova, Gene networks controlling early cerebral cortex arealization. *Eur J Neurosci,* **23**(2006) 847–856.

[2] O Schmitt, M Pakura, T Aach, M Böhme, Analysis of nerve fibers and their distri-bution in histologic sections of the human brain. *Micr Res Tech,* **63(**2004**)** 220–243.

[3] K Amunts, K Zilles, Advances in cytoarchitectonic mapping of the human cerebral cortex. *Neuroimg Clin N Am*, **11**(2001) 151–169.

[4] O Schmitt, M Böhme, A robust transcortical profile scanner for generating 2D-traverses in histological sections of rich curved cortical courses. *NeuroImage,* **16**(2002) 1103–1119.

[5] A Schleicher, K Amunts, S Geyer, P Morosan, K Zilles, Observer independent method for microstructural parcellation of cerebral cortex: a quantitative approach to cytoarchitectonics. *NeuroImage,* **9**(1999) 165–177.

[6] O Schmitt, L Hömke, L Dümbgen, Detection of cortical transition regions utilizing statisti-cal analyses of excess masses. *NeuroImage,* **19**(2003) 42–63

[7] O Schmitt, J Modersitzki, S Heldmann, S Wirtz, L Hömke, W Heide, D Kömpf, A Wree. Three-dimensional cytoarchitectonic analysis of the posterior bank of the human precentral sulcus. *Anat Embryol,* **210**(2005) 387–400.

[8] B Jähne, Practical Handbook on Image Pro-cessing for Scientific and Technical Appli-cations. CRC Press, (2004) Boca Raton.

[9] P Perona Orientation diffusions. *IEEE Trans Im Proc,* **7**(1998) 457–467.

[10] P Perona, J Malik, Scale space and edge detection using anisotropic diffusion. *Pat Anal Mach Intel,* **12**(1990) 629–639.

[11] A Schleicher, K Amunts, S Geyer, T Kowalski, T Schormann, N Palomero-Gallagher, K Zilles, A stereological approach to human cortical architecture: identification and delineation of cortical areas. *J Chem Neuroanat,* **20**(2000) 31–47.

[12] G Granlund., H Knutson, Signal processing for computer vision. Kluwer Academic Publishers, (1995) Dordrecht.

[13] J Bigün, G Granlund, Optimal orientation detection of linear symmetry. *Proc ICCV*, (1987) 433–438.

[14] J Horton, D Adams, The cortical column: a structure without a function. *Phil Trans R Soc B,* **360**(2005) 837–862.

[15] J Weickert, Anisotropic diffusion in image processing. Teubner, (1998) Stuttgart.

[16] J Weickert Coherence-enhancing diffusion filtering. *Int J Comp Vis,* **31**(1999) 111–127.

[17] A Rao, B Schunck, Computing oriented texture fields. *CVGIP: Graph. Models Image Process*. **53**(1991), 157–185.